Physical Processes Governing the Rapid Deepening Tail of Maritime Cyclogenesis

PAUL J. ROEBBER AND MELISSA R. SCHUMANN

Atmospheric Science Group, University of Wisconsin—Milwaukee, Milwaukee, Wisconsin

(Manuscript received 3 October 2010, in final form 6 April 2011)

ABSTRACT

The positively skewed distribution of maritime cyclone maximum deepening rates is investigated for cyclones as a class rather than through individual case study, using a series of experiments employing perpetual January simulations from the global version of the fifth-generation Pennsylvania State University–NCAR Mesoscale Model (MM5). The relative roles of latent heat release, baroclinic instability, and boundary layer friction in producing this tail behavior are elucidated. The experiments reveal that the strongest maritime storms are the result of the baroclinic dynamics of the relative few being preferentially enhanced through feedback with the available moisture. Strong baroclinic forcing, in the absence of this moisture availability and resultant latent heating, does not produce the skewed rapid deepening tail behavior. An increase in surface roughness and accompanying friction in the maritime region provides only a slight brake on cyclone development. The results support previous research that argued that the rapid deepening tail is evidence of a fundamentally distinct pattern of behavior characteristic of maritime cyclones compared to continental systems, and that this behavior is the result of process interactions (baroclinic dynamics and latent heat release) rather than the nature of the data.

1. Introduction

Sanders and Gyakum (1980) extensively investigated rapidly developing maritime cyclones and their work inspired much observational and modeling research dedicated to understanding the dynamics of these systems [see Uccellini (1990) for a comprehensive review]. Roebber (1984) tracked midlatitude cyclones in a large portion of the Northern Hemisphere for a single year and showed that the statistical distribution of cyclone deepening rates is skewed toward rapid development. Gyakum et al. (1989) followed that analysis and reproduced the rapid deepening tail of Roebber (1984) for an 8-yr sample of North Pacific storms (Fig. 1 of this paper, except with an additional 2 yr of data; see below). For the 10-yr sample of Fig. 1, the Kolmogorov–Smirnov test (e.g., Roebber 1989) allows for rejection of the null hypothesis that these data are drawn from a normal distribution ($p = 0.04$).

Corresponding author address: Paul J. Roebber, Atmospheric Science Group, Dept. of Mathematical Sciences, 3200 North Cramer Ave., Milwaukee, WI 53211.
E-mail: roebber@uwm.edu

DOI: 10.1175/MWR-D-10-05002.1

Roebber (1984, 1989) argued that this rapid deepening tail is evidence of a fundamentally distinct pattern of behavior characteristic of maritime cyclones compared to continental systems, that this distinction holds across a wide spectrum of storm intensities, and that this behavior relates to physical processes rather than the nature of the data. For example, Roebber (1989) showed that warm season cyclones exhibit a similar rapid deepening tail, but with a distribution shifted toward less development. Rapidly deepening storms are of practical importance since, for example, 93% of the rapid deepeners of the Roebber (1984) dataset, defined as meeting or exceeding the 1-Bergeron criterion [latitude-adjusted storm central pressure falls of at least 24 hPa in 24 h; see Sanders and Gyakum (1980), Roebber (1984), or Roebber (1989) for further details], achieve central pressures at some point in their history that are below the median for all cyclones.

Considerable case-based research has led to the present understanding that rapidly developing systems owe their intensity primarily to the interaction between adiabatic processes and the diabatic process of latent heat release (e.g., Uccellini 1990; Bosart 1999 and references therein) over short intervals (e.g., Roebber

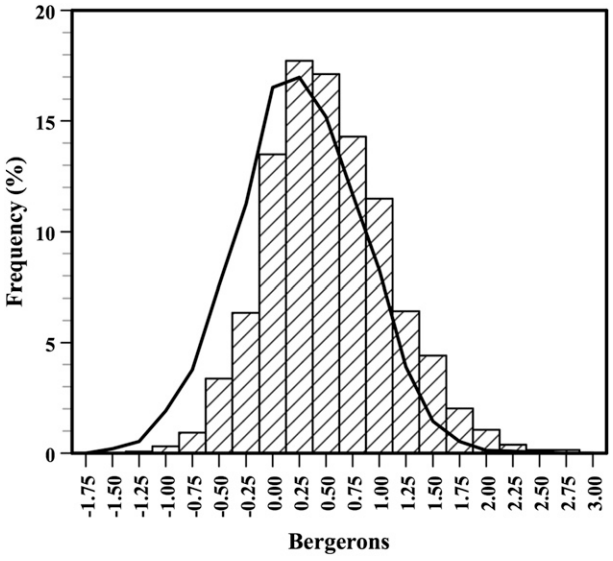

FIG. 1. Observed 24-h maximum deepening (Bergerons) for Pacific maritime cyclones from the augmented Gyakum et al. (1989) dataset. Counts are expressed as frequencies (%). The best-fit normal distribution curve, fixed to the mode of the observed distribution, is also shown.

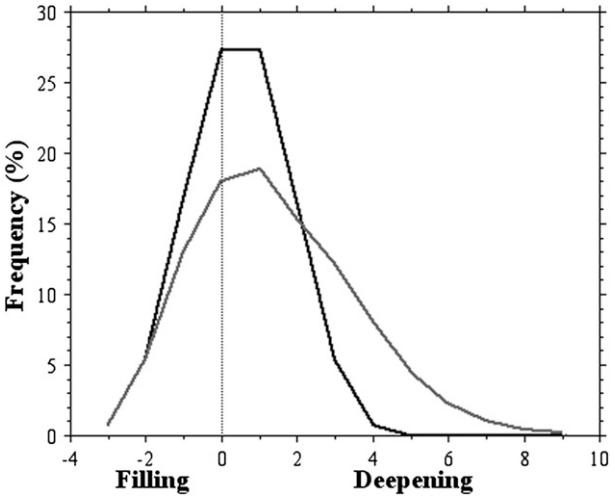

FIG. 2. Hypothetical deepening rate distributions (frequencies) for cyclones undergoing development through normally distributed baroclinic processes (black; X_0 of Table 1), and baroclinic and latent heat release interaction (gray; fX_0 of Table 1).

1984). For example, Kuo et al. (1991) found in a model simulation of a specific case that moist frontogenesis, in addition to amplifying the adiabatic circulation, established a positive feedback between baroclinic and diabatic effects by producing strong low-level convergence in the precipitation zone. This influence, however, is not simple. Kuo and Low-Nam (1990) and Kuwano-Yoshida and Asuma (2008), for example, found that the relative importance of latent heat release varied substantially across a number of rapid development cases, with the latter authors showing that mesoscale details such as frontal structure and jet stream configuration are important to the distribution of this diabatic heating and its influence on development.

To understand how interactive physical processes might produce a skewed deepening tail, consider a normal distribution of cyclone deepening that might result from baroclinic instability (Fig. 2). In that case, there is no skewness toward the rapid deepening tail. Further, increases in baroclinic dynamics, as might be present in the zone between the warm, western boundary currents of the Pacific and Atlantic Oceans and the upstream continents, would produce larger deepening rates, but again no skewness. In either scenario, the strongest storms will appear exceptional, but with a stretched deepening tail, the ''distance'' between the norm, defined by some measure of where the largest frequency of developing cyclones occurs, and these storms, is larger.

Within the quasigeostrophic framework, latent heat release can be parameterized according to the rate of change of saturation specific humidity following the saturated, ascending motion produced by adiabatic processes. In that case, the total vertical motion and associated surface pressure tendencies are proportional to the ''forcing'' from adiabatic processes, modified by an effective static stability, which is always smaller for saturated ascent (e.g., Krishnamurti 1968; Tracton 1978). In this case, there is an ''amplification factor'' that multiplies the adiabatic development rate, producing a distribution skewed toward rapid deepening (Fig. 2; Table 1), as is in fact observed (Roebber 1984, 1989; Gyakum et al. 1989; Fig. 1). The

TABLE 1. Percentile distributions generated from a random, normal distribution with mean 0.50 and standard deviation 1.00 (X_0), the product of X_0 with an amplification factor f (which itself has a gamma distribution with shape parameter 2, such that the median value of f is 1.20), and the product of X_0 with a constant amplification factor $c = 2.20$. To simulate saturated ascent, the amplified distributions are set to $(1 + f)X_0$ and cX_0 for X_0 positive, otherwise X_0. Note the stretching of the ''deepening tail'' of the product distributions relative to the normal distribution, as indicated by the 75th and 90th percentile values. Also shown is the skewness for each distribution.

Percentile	X_0	$(1 + f)X_0$	cX_0
10	−0.79	−0.79	−0.79
25	−0.18	−0.18	−0.18
50	0.50	1.13	1.10
75	1.17	2.68	2.58
90	1.78	4.10	3.91
Skewness	0.00	1.03	0.60

strongest storms appear in a sense as ''lucky'' accidents in which the dynamics of these relative few have been somehow enhanced. Note that this skewness will result regardless of the distribution of the amplification factor, including a constant value (see Table 1).

This idea of process interaction, however, has not been validated for rapid deepening cyclones *as a class* and the direct influence of specific physical processes on this tail behavior has not been investigated. For example, what are the relative roles of latent heat release, baroclinic instability, and reduced boundary layer friction in producing the rapid deepening tail? In this paper, these ideas are explored through the use of global numerical model experiments, as described in section 2. The results of these experiments are presented and synthesized within the context of the available literature in section 3, while a concluding summary is provided in section 4.

2. Methods

a. Global model

Sanders and Mullen (1996) showed that the National Center for Atmospheric Research (NCAR) Community Climate Model (CCM2) is able to reproduce important characteristics of Northern Hemispheric rapidly developing cyclones, including both their overall intensity and primary location along the east coasts of North America and Asia. The equivalent grid spacing of this spectral model is approximately 200 km, scales consistent with earlier research findings in which the full development of rapidly deepening cyclones were first obtained (Sanders 1987). Dudhia and Bresch (2002) reported on the availability of a global version of the fifth-generation Pennsylvania State University (PSU)–National Center for Atmospheric Research (NCAR) Mesoscale Model (MM5), with two hemispheric domains of 120-km grid spacing at 60°N (and 60°S). Those authors showed through a variety of experimental trials that the simulations produced by this global version of MM5 were realistic and that this setup can be used as an alternative kind of climate model.

These two developments provide an opportunity to directly address the issue of the rapid deepening tail as discussed in the previous section. Four 320-day,[1] perpetual January simulations are produced with the goal of exploring the physical processes governing the rapid deepening tail behavior. The first 10 days in each experiment are thrown out to allow for model spinup, leaving 310 days (i.e., the equivalent of 10 Januarys) for analysis. All experiments use standard physics [simple ice (Dudhia 1989), Grell cumulus parameterization (Grell et al. 1994), Blackadar planetary boundary layer (Blackadar 1979; Zhang and Anthes 1982), and a rapid radiative transfer model (Mlawer et al. 1997); see Dudhia and Bresch 2002 for additional details] but adjustments to moisture availability (and consequently latent heating), solar radiation (and consequently baroclinicity), and surface roughness (and consequently friction) are made to test ideas concerning the tail behavior, as described below.

The first experiment follows the basic model setup (hereafter, CONTROL). The goal of this experiment is to verify that the observed cyclone climatology (spatial distribution, relative intensities, and rapid deepening tail) is reasonably represented by the model and to provide a baseline of comparison for subsequent simulations. For the second experiment, moisture availability over the oceans is reduced from 100% to 30% (hereafter, reduced latent heat release or RLHR), approximating the average value over land surfaces. This is accomplished through the surface moisture flux parameterization, after Carlson and Boland (1978), which is directly proportional to the surface moisture availability. This change results in a 50% reduction in peak latent heat flux over the oceans relative to CONTROL (not shown). If latent heat release is a key contributor to the rapid deepening tail as case study research suggests, and if the latent heating acts interactively to enhance the baroclinic response in these storms as argued in section 1, then one expects a reduction in skewness of the deepening distribution to occur in this experiment.

For the third experiment, the model setup is the same as RLHR except that, in addition, the solar flux (received at the top of the atmosphere) is increased by 1.4 W m^{-2} or approximately 0.1% (hereafter, reduced latent heat release and enhanced radiation or RLHR/RAD). This adjustment leads to a 7% increase in the midlatitude, Northern Hemispheric mean zonal wind speed relative to CONTROL over the course of the simulation (Fig. 3). This experiment attempts to address the question as to whether enhanced baroclinicity (as represented by the increase in mean zonal wind; but see below) in combination with some latent heating is the functional equivalent of baroclinic storms developing within the context of moisture-rich, maritime environments in which latent heating is abundant.

The fourth and final experiment returns to the setup of CONTROL except that the roughness length over the

[1] For the ROUGH experiment, computer hardware problems resulted in a slightly shorter simulation, providing 280 rather than 310 days for analysis.

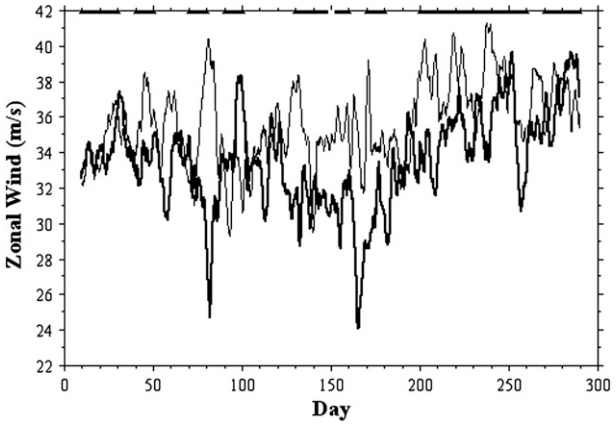

FIG. 3. Mean hemispheric zonal wind (m s^{-1}) in the latitude band 30°–50°N for CONTROL (thick) and RLHR/RAD (thin) for days 10–290 of the simulations. Also shown are the 10-day periods for which the Eady growth rate maximum in the Pacific storm track entrance region exceeds the average value of CONTROL.

water is increased to 10 cm (hereafter, ROUGH), approximating an average winter value over land surfaces (e.g., grassland). This adjusts the overwater roughness from a variable quantity proportional to the square of the friction velocity, which for neutral conditions produces roughness lengths of the order of 0.1–1 cm for winds of 10–30 m s^{-1}. Even for winds as high as 50 m s^{-1}, a 10-cm roughness length is more than twice the usual value. Thus, if reduced friction is an important contributor to the rapid deepening tail of maritime cyclones, then the result of this increased friction should be reduced skewness in the maximum deepening distribution in this sample of maritime storms. Note that we have reversed the question, in some sense, by increasing friction over the oceans, to maintain the focus on maritime cyclones and to assure that there will be a large sample of storms to analyze.

In following a global modeling rather than case study approach, as in past work, there is a confounding influence that must be considered. It may be that the changes in moisture availability, solar radiation, and surface roughness will impact the large-scale flow and thus complicate interpretation of cyclone-scale effects. For example, some studies have suggested that midlatitude latent heating has a substantial impact on the cold-season stationary waves, and that this storm track heating may be crucial to maintaining high baroclinicity over the storm track entrance region (Hoskins and Valdes 1990; Held et al. 2002). Thus, if RLHR results in a substantial decrease in baroclinicity, then reductions in the rapid deepening tail may be the result of this indirect interaction rather than the direct interactions of interest in this paper.

TABLE 2. Experimental results for Pacific maritime cyclones. Shown are the Eady growth rate maximum (σ_{BI}; day^{-1}) in the Pacific storm track entrance region, the number of Pacific maritime cyclones N, the rate of cyclone occurrence (rate; day^{-1}), the mean, median, and mode of deepening rate (Bergerons, where positive indicates deepening), and the moment-based skewness (Sk; boldface indicates greater than two standard errors of skew beyond zero). Mode is computed using a bin interval of 0.125 Bergerons [3 hPa (24 h)$^{-1}$]. Data are from the manual analysis, and the four model experiments, where the RLHR/RAD is subsampled in 10-day periods as a function of the value of the Eady growth maximum (see text for details).

Dataset	σ_{BI}	N	Rate	Mean	Median	Mode	Sk
Manual	—	2514	1.38	0.53	0.47	0.25	**0.39**
CONTROL	2.03	260	0.84	0.70	0.62	0.56	**0.43**
RLHR	2.12	224	0.72	0.82	0.81	0.75	0.11
RLHR/RAD	>2.03	135	0.80	0.81	0.72	0.63	0.14
ROUGH	2.17	232	0.83	0.73	0.69	0.75	**0.28**

To evaluate this issue, the Eady growth rate maximum σ_{BI} is calculated in the storm track entrance region as a measure of baroclinicity (e.g., Hoskins and Valdes 1990). We define σ_{BI} at 2 km above sea level as

$$\sigma_{BI} = 0.31 f \left| \frac{\partial v}{\partial z} \right| N_b^{-1}, \quad (1)$$

where f is the Coriolis parameter, v is the zonal wind, and N_b is the Brunt–Väisälä frequency. Vertical derivatives in (1) are computed with a centered finite difference using a 500-m height increment. We define the Pacific storm track entrance region as the area bounded by 30°–45°N and 135°–165°E. This measure of baroclinicity changes rather moderately between the experiments, except in RLHR/RAD, where it falls from 2.03 day^{-1} in CONTROL (Table 2) to 1.81 day^{-1}.

That the small imposed increase in the solar constant results in substantial and somewhat contrary changes in the flow (i.e., an increase in midlatitude, Northern Hemispheric mean zonal flow but a decrease in baroclinicity over the Pacific storm track entrance region) is surprising. Figure 3 shows that the connection between the hemispheric flow and that in the region of the Pacific storm track is highly variable. The total number of cyclones across the hemisphere, for example, increases 3% in RLHR/RAD relative to CONTROL, consistent with the hemispheric increase in zonal wind, but the number of *Pacific* cyclones decreases in RLHR/RAD by 11%, consistent with the average decrease in baroclinicity there. The temporal variability, however, suggests an opportunity to stratify RLHR/RAD into periods for which the Eady growth rate maximum is larger than that of the average value of CONTROL, and report those

results separately, as a means of detecting the impact of enhanced baroclinicity.

The reasons why a small change in solar radiation can have these sizeable impacts on the model flow are somewhat beyond the scope of this paper, but there are some research results reported elsewhere that bear on this question. Haigh et al. (2005) demonstrate, using a simplified global circulation model, that heating of the lower stratosphere affects the meridional extent and strength of the Hadley cell and, consequently, the position and strength of the zonal jets. Haigh (2009) reviews the literature and documents that small changes in solar radiation can induce a detectable response in the lower-tropospheric circulation. Kurz (2009) found, in experiments with solar radiation in the MM5, results consistent with the findings of Haigh et al. (2005). Although Haigh et al. (2005) show a weakening of the subtropical jet, there is some suggestion that increased solar radiation leads to a net strengthening of the midlatitude zonal jet, particularly poleward of 40°N.

Another concern is changes in low-level moisture resulting from the reduced latent heat, and the corresponding potential impacts of a reduced ''greenhouse effect'' on the model climate. In RLHR and RLHR/RAD, as noted above, moisture availability is reduced by 70% over the oceans with a concomitant reduction in surface moisture flux. In RLHR, North Pacific precipitable water is 5% below that of CONTROL, leading to reductions in low-level potential temperature (1.5 km above sea level) of 0.9°C in the region. Despite this, the Eady growth rate maximum suggests that baroclinicity in this simulation is comparable to that of CONTROL (Table 2).

In ROUGH, the increased roughness length, in addition to directly affecting the surface stress, influences surface heat and moisture fluxes in a complicated fashion through changes in the friction velocity (e.g., Carlson and Boland 1978). Thus, this experiment is not exclusively a test of enhanced friction over the oceans, although the change in precipitable water over the Northern Hemispheric ocean basins relative to CONTROL is less than 1%. Changes in baroclinicity in the Pacific storm track entrance region are somewhat larger (+6.8%; Table 2), although as will be discussed below, such changes appear to relate only in a complex fashion to cyclone activity and in no clear way to rapid development.

b. Cyclone tracking

In many cyclone studies, the labor-intensive process of manual analysis has been used to track storms and/or document development (e.g., Petterssen 1956; Klein 1957; Reitan 1974; Colucci 1976; Zishka and Smith 1980; Sanders and Gyakum 1980; Whittaker and Horn 1981; Roebber 1984; Gyakum et al. 1989). In recent years, the availability of large datasets obtained from reanalyses and climate simulations has rendered manual tracking less feasible. Accordingly, a variety of automated methods have been developed and are now widely used.

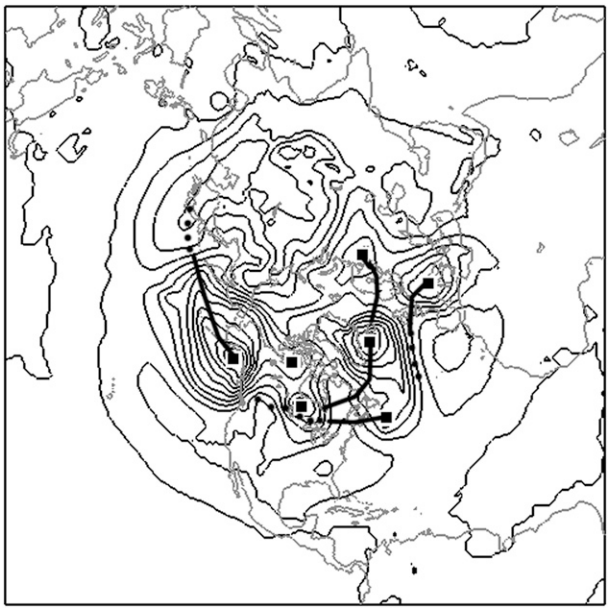

FIG. 4. Cyclone tracks produced by the automated system over a 5-day period in CONTROL. Shown are the sea level pressure analysis on day 5 (8-hPa interval), day 5 cyclone centers identified by the automated system (black squares), automated cyclone tracks (solid lines), and missed tracks as determined by manual inspection (dots).

Both manual and automated approaches use rules to identify cyclones on a given map and then to maintain the continuity of cyclones across a set of map times. Manual cyclone tracking involves some subjective decision making based upon synoptic experience concerning cyclone behavior and dynamics, particularly with respect to the continuity of an existing cyclone when the system may not be well developed. It is not straightforward to construct a concise set of rules that captures this process and as a result, different automated methods have been developed. In this paper, because of the large number of days across four simulations, an automated cyclone identification and tracking algorithm (based on local maxima in geostrophic vorticity and temporal continuity) is employed to determine cyclone histories for all simulations.

An example of cyclone tracks produced over 5 days using the automated method (Fig. 4) demonstrates both the capabilities and the limitations of this system. A total

of eight cyclones of duration of at least 24 h were identified both manually and with the automated tracking system during this period (seven are apparent on day 5). The automated system, however, missed the initiation of four of these storms (see dots in Fig. 4). Two of these partial tracks were for cyclones that later became rapid deepeners, but in neither of these cases was the most rapid deepening phase missed.

Since we are concerned with tail behavior, however, it is important to ascertain to what degree this methodology will influence our ability to detect differences between the experiments. Raible et al. (2008) compared several automated cyclone identification and tracking methods and found that variations are primarily related to cyclone track length, as suggested by Fig. 4. Blender and Schubert (2000) and Jung et al. (2006) show that coarse temporal and spatial data exacerbate tracking difficulties connected to automated methods. The 6-hourly, 120-km grid space data used here, however, are sufficient to limit this problem. Smith et al. (2011, manuscript submitted to *Mon. Wea. Rev.*, hereafter SRG) compared contemporaneous 10-yr North Pacific cyclone datasets derived from automated and manual tracking and identified a cyclone underdetection problem in the automated method, most particularly for cyclones early in their life histories (such as waves), a result consistent with that shown for the 5-day period in Fig. 4. In contrast, the automated method matched the manual results well in detecting and tracking mature cyclones. Despite this, some reduction in the automated detection of rapid deepening events was noted, owing to discontinuities in cyclone track histories related primarily to coarse grid resolution. Thus, statistics dependent on cyclone redevelopment, such as often occurs in association with western ocean warm currents, and rapid developments early in the history of a cyclone might be affected.

SRG determined that the net effect of these detection-and-tracking errors was to underdetect cyclones fairly uniformly across all *deepening rates*, and to decrease skewness in the maximum deepening rate distribution of maritime systems in that sample. In the present study, the sea level pressure data are available at twice the temporal frequency (6 hourly rather than 12 hourly) and higher spatial resolution (120-km grid spacing at 60°N rather than 2.5° × 5° latitude–longitude), and the detection-and-tracking method has been calibrated to this model resolution as recommended by SRG. Accordingly, in the analysis that follows, while we expect some cyclone underdetection to occur (e.g., Fig. 4), the impacts on rapid deepening statistics should be relatively small, conservative in the sense of underestimating skewness, and equally applicable to all experiments.

In this study, we use the traditional moment measure of skewness, written as

$$\mathrm{Sk} = \frac{\frac{1}{N}\sum_{N}(x_i - \bar{x})^3}{\left[\frac{1}{N}\sum_{N}(x_i - \bar{x})^2\right]^{3/2}}, \tag{2}$$

where N is the sample size and the overbar represents the sample mean. The standard error of skew for this measure (Tabachnick and Fidell 2007) is

$$\mathrm{se} = \sqrt{\frac{6}{N}}. \tag{3}$$

To detect whether skew deviates significantly from zero (that of a normal distribution), we will follow the usual practice of requiring that Sk exceed two standard errors.

We return to the arguments used in constructing Fig. 2 and Table 1 to assess the influence of sample size on detecting a real difference in skewness from that of a normal distribution. We generate two random distributions of sample size M, the first from a normal population with mean 0.5 and standard deviation 1.0, and the second as in Table 1, but for a range of amplification factors, producing skewness ranging from 0.22 to 0.63. We repeat this 1000 times for each distribution size M and each amplification factor. We then compute the confidence limit of detecting the nonnormality of the skewed distribution by counting the number of times that the computed skewness difference exceeds two standard errors. This analysis produces a power law pattern of behavior of the form

$$M_{95} = 113.458\mathrm{Sk}^{-1.329}, \tag{4}$$

where M_{95} is the minimum sample size required to produce detectable skewness differences at the 95% level.

The salient point for this study is that distributions with low skewness (e.g., Sk = 0.22) will require a sample size more than 4 times that needed for a distribution with high skewness (e.g., Sk = 0.63). For observed cyclone deepening distributions with skewness of $O(0.45)$, this law suggests that we will need a sample with several hundred cyclones to reliably differentiate it from a normal population. Since (4) is empirical and was developed from an assumed distribution form, these sample size estimates are approximate, but can be used to help inform the reliability of our conclusions and suggest future improvements. We will return to this topic in the concluding discussion.

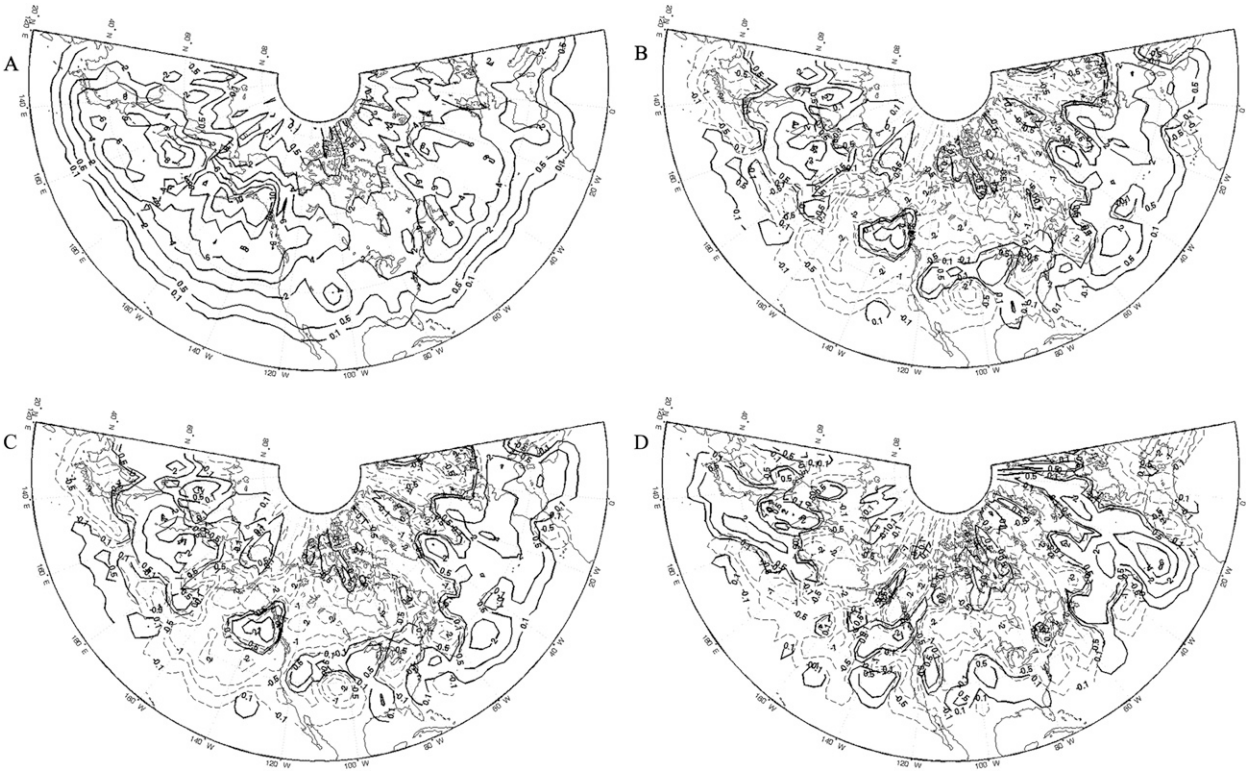

FIG. 5. Simulated cyclone frequencies, counted in area-weighted 2.5° latitude–longitude tesserae. Contours are smoothed using a five-point smoother. Counts are shown for (a) CONTROL, (b) RLHR minus CONTROL, (c) RLHR/RAD minus CONTROL, and (d) ROUGH minus CONTROL.

3. Results and synthesis

Before turning to the main issue of rapid deepening, we first compare maps of cyclone frequencies from each of the four simulations, to gain a sense of the resultant cyclone climates (Fig. 5). Notably, CONTROL shows structures familiar from observed climatologies: high cyclone frequencies along the western boundary currents, that is, the Kuroshio in the Pacific, extending across that basin to dissipation in the Gulf of Alaska; the Gulf Stream in the Atlantic, extending northeastward to the Icelandic low; and with lee cyclogenesis east of the Rocky Mountains of Colorado and Wyoming (Fig. 5a).

Difference maps for NLHR and for NLHR/RAD are quite similar and suggest a northward displacement of the storm track leading to eventual cyclone dissipation in the Gulf of Alaska (Figs. 5b and 5c). There is some evidence that this displacement continues across North America, where lee cyclogenesis also appears farther to the north than in CONTROL. We speculate that with the loss of substantial latent heating in these runs relative to CONTROL, cyclone development is more closely tied to the main axis of the baroclinic zone. In the Atlantic, however, differences do not continue to show a northward displacement. Rather, there is generally increased cyclone activity relative to CONTROL, with the notable exception of the key region for rapid deepening offshore of Nova Scotia, and some suggestion of greater meridional orientation of the storm track.

In ROUGH, the cyclone activity along the Kuroshio is increased, as are the North American lee cyclones (Fig. 5d). There is, however, a substantial reduction in cyclone activity along the Gulf Stream relative to CONTROL, again with implications for rapidly deepening cyclones. The primary conclusions are that CONTROL appears to reasonably represent observed cyclone activity, and that the cyclone climatologies resulting from the three physics runs are distinct from CONTROL and from each other, with the exception of RLHR and RLHR/RAD, which exhibit very similar gross structures.

The differences in cyclone activity in the Pacific and Atlantic basins require further investigation, and invite comparison with manual analyses. Calculations of the Eady growth rate maximum for the storm track entrance regions of both the Pacific (Table 2) and Atlantic (not shown) indicate, as in the above qualitative discussion, that there is considerably more run-to-run variability in baroclinicity in the Atlantic basin, and that the cyclone

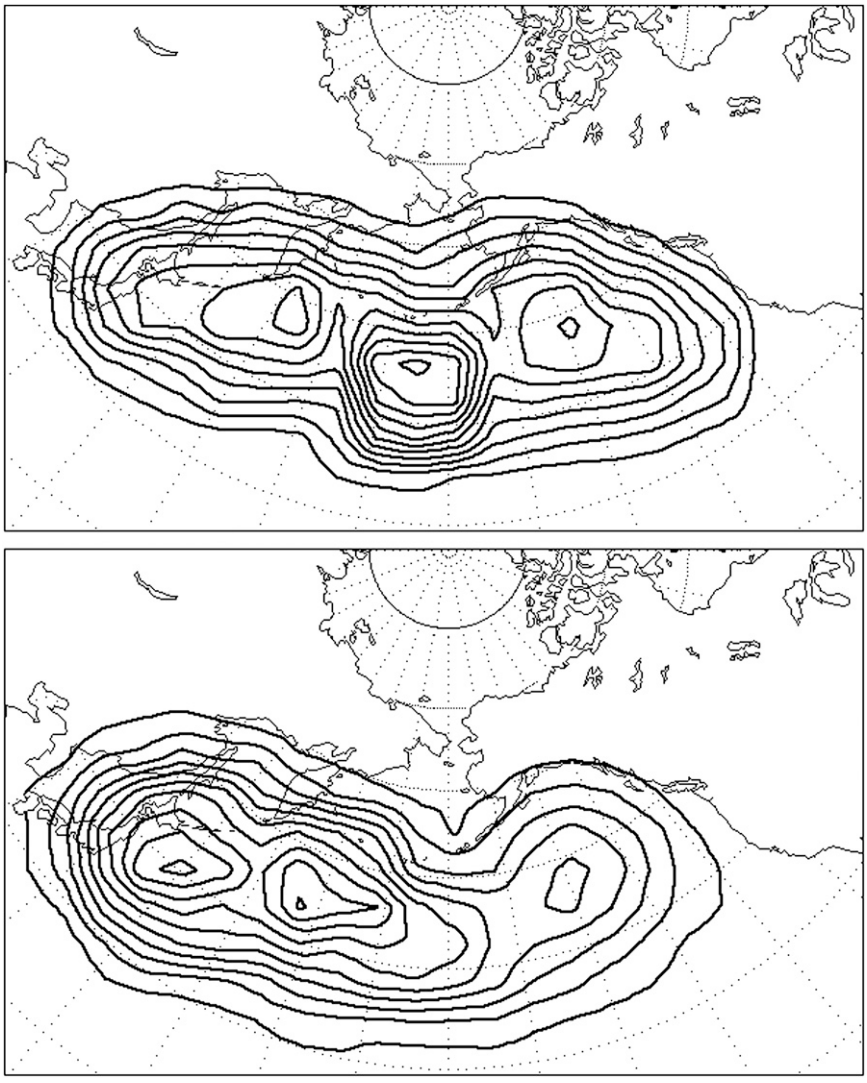

FIG. 6. Smoothed counts of maximum deepening position for rapid deepening cyclones (greater than or equal to 1 Bergeron) in (top) CONTROL and (bottom) manual analysis data (see text for details). Contour interval of 1, normalized to 10 cold seasons as in the manual dataset. Latitude–longitude is shown on a 10° × 10° grid, oriented with respect to 170°W.

activity does not necessarily correlate between the two basins. As such, and owing to the existence and availability of a 10-yr manual cyclone tracking climatology for the North Pacific, henceforth we will consider only Pacific storms in the analysis (defined as the region from 30° to 60°N and 140°E to 130°W).

The manual analysis is that of Gyakum et al. (1989), augmented with an additional two cold seasons (1 October–31 March), for the period of 1975–85. In the manual analysis, a cyclone center is defined by at least one closed 4-hPa contour around a sea level pressure minimum for at least one time, obtained from the National Meteorological Center's [NMC, now known as the National Centers for Environmental Prediction (NCEP)] 6-hourly Northern Hemisphere final analysis surface charts (Corfidi and Comba 1989). Positions were recorded at 0.5° latitude–longitude resolution and a cyclone was tracked provided it existed for at least 12 h (i.e., at least three consecutive NMC 6-h analyses).

The maximum deepening positions for all storms exceeding 1 Bergeron in CONTROL (Fig. 6, top) compare favorably to the observations (e.g., Fig. 7c of Roebber 1984). Key similarities include the three local maxima within the western Pacific, along the date line and near the Gulf of Alaska, and the higher frequencies along the Gulf Stream current (not shown). To make this comparison more explicit, however, we plot the 10-yr manual dataset using the same conventions (Fig. 6, bottom).

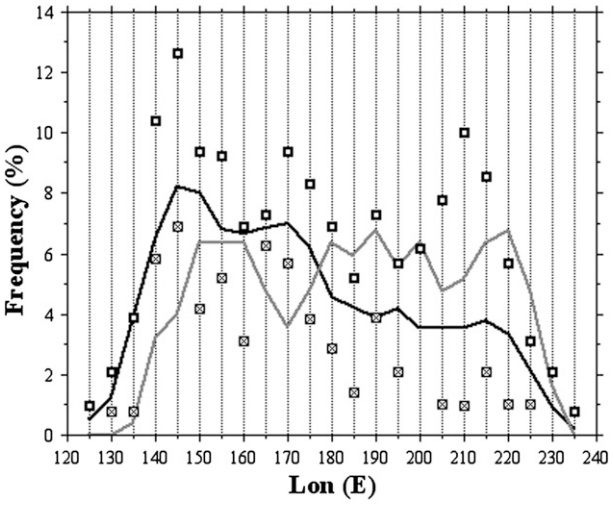

FIG. 7. Longitudinal frequency (% of entire sample) of rapidly deepening cyclones in the 30°–60°N band from the manual dataset (black) and CONTROL (gray). Also shown are the maximum (open square) and minimum (checked square) biennial frequencies in the 10-yr manual dataset for each 5°-longitude bin.

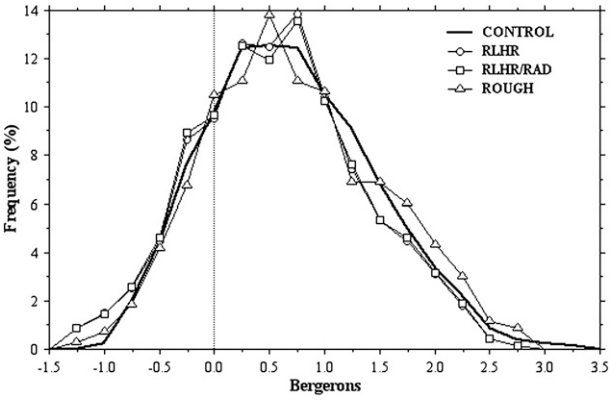

FIG. 8. The 24-h maximum deepening (Bergerons) for Pacific maritime cyclones from the CONTROL, RLHR, RLHR/RAD, and ROUGH simulations. Counts are expressed as frequencies (%). The RLHR and RLHR/RAD distributions are slid one deepening bin to the left for comparative purposes (see text for details).

Although the qualitative similarity is substantial, also apparent is a low (high) bias relative to the manual analysis in the western (eastern) Pacific.

Since the CONTROL simulation occurs over 310 cold-season days versus 1822 for the manual analysis, even when discounting cyclone underdetection, there may be an impact from sampling variability. Figure 7 quantifies the aforementioned low-to-high cyclone bias proceeding from west to east across the Pacific basin, but also strongly suggests that sampling variability cannot be discounted as an explanation. Perhaps more significantly, the cyclone detection biases noted by SRG operate in this same direction, preferentially missing the early stages of developing cyclones in the western Pacific, and identifying them and others at the mature stage in the eastern ocean. Thus, the differences noted here likely do not result from model deficiencies and suggest that our proposed methodology, taking into consideration the impacts of these limitations, is feasible.

The distribution of maximum deepening for maritime storms from CONTROL (Table 2; Figs. 1 and 8) exhibits the characteristic skewness toward rapid deepening (Roebber 1984; Gyakum et al. 1989) and includes peak events of $O(3)$ Bergerons, consistent with the observations (e.g., Sanders and Gyakum 1980). As expected, however, the rate of cyclone detection is less than in the manual analysis and the distribution is shifted more strongly toward deepening (e.g., SRG). The preservation of the relative ''shape'' of the distribution as measured by the skewness, despite this distribution shift, is important as it confirms the utility of skewness as an appropriate measure. Although our model experiments will be compared to CONTROL rather than manual data, using the same automated cyclone tracking methodology, overall distribution shifts might also occur owing to changes in baroclinicity or other climatic features, factors that we can monitor but not fully control in the experimental design. These will be noted as appropriate.

Next, we discuss the results from the full suite of experiments (Table 2). The null hypothesis of RLHR, that the reduced latent heat will have no impact on the rapid deepening tail of maritime storms (i.e., the distribution of maximum deepening will remain skewed) is rejected. The skewness is substantially reduced relative to CONTROL and is no longer significantly different from zero, based on two standard errors, even though the environment, as measured by σ_{BI}, was more strongly baroclinic and the deepening rate distribution (mean, median, and mode) shifted toward development. Latent heat release, as suggested by the research on individual cyclones and in the statistical–theoretical arguments provided here, has a stretching effect on maritime cyclone development and this effect is readily detectable in the overall deepening distribution.

As noted in section 2a, σ_{BI} falls overall in RLHR/RAD relative to CONTROL, but we stratify this run into 10-day periods according to enhanced or reduced baroclincity relative to the average value of CONTROL (σ_{BI} greater or less than 2.03, respectively), as indicated in Fig. 3. As noted previously, enhanced baroclinicity is associated with greater cyclone activity (18% more than for σ_{BI} less than 2.03). This does not correlate directly with intensity, however, with the mean and median deepening being somewhat larger for the less baroclinic

periods of this simulation. The null hypothesis of RLHR/RAD, that reduced latent heat combined with enhanced baroclinicity will have no significant effect on the rapid deepening tail of maritime storms, is rejected. Although the overall distribution is shifted toward stronger development, as with RLHR, the skewness is statistically indistinguishable from that of a normal distribution. It would appear that it is the process of latent heating acting in concert with baroclinicity that generates the rapid deepening tail and resulting skewness. Increased baroclinicity, as occurred in both RLHR and the subsample of RLHR/RAD, can increase development but does not affect the stretching of the distribution tail.

The null hypothesis of ROUGH, that increased roughness over the oceans and the resulting friction, will have no significant effect on the rapid deepening tail of maritime storms (i.e., the distribution will remain skewed toward rapid development) cannot be rejected based upon skewness. Indeed, the cyclone frequency and median deepening in this experiment are similar to CONTROL, and while skewness is reduced, it is still significant. We conclude that while reduced friction over the oceans can contribute to rapid deepening, this process is a second-order effect.

Finally, to gain a physical perspective on the relative contributions of baroclinic processes and latent heat release on the development of cyclones on the rapid deepening tail, we form composites from a sample of CONTROL (Fig. 9) and RLHR/RAD (Fig. 10) cases. To produce comparable samples for compositing, we select 10 of the top 11 most rapid deepeners from CONTROL and the 10 most rapid deepening storms from the subsample of RLHR/RAD. These cases had 24-h deepening rates for CONTROL (RLHR/RAD) of 2.79 (2.71), 2.50 (2.50), 2.40 (2.36), 2.33 (2.35), 2.32 (2.27), 2.25 (2.26), 2.22 (2.17), 2.12 (2.07), 2.07 (1.99), and 2.06 (1.98) Bergerons, for a sample mean deepening rate of 2.31 (2.27) Bergerons. Evidence of strong baroclinic dynamics in both composites is provided by 500-hPa cyclonic vorticity advection and the left exit region of the 300-hPa jet streak positioned above the surface cyclone center (Figs. 9 and 10). We note that the composite upper-level jet streak is stronger and the composite 500-hPa trough is sharper in RLHR/RAD, while the composite 24-h precipitation amount is 12% larger over and downstream of the surface cyclone center in CONTROL, with some evidence of a diabatic response with enhanced thickness ridging there.

It would appear, then, that the distinctions between maritime and continental cyclogenesis and the resulting deepening distributions documented in the literature (Roebber 1984, 1989; Gyakum et al. 1989) are indeed driven primarily by feedbacks between baroclinic and diabatic processes (latent heat release), with a small contribution from reduced friction over the oceans. It is notable that an increase in baroclinic forcing alone (i.e., in the absence of substantial latent heat release) is not effective in producing rapid development across cyclones as a class (since certainly, in individual cases, this can occur; e.g., a 2.71-Bergeron storm was produced in RLHR/RAD). Continental cyclogenesis occurs with baroclinic forcing but with limited contributions from diabatic processes, while friction plays a nonnegligible but secondary role in providing a brake on development, resulting in the essentially Gaussian character of the deepening distributions of those storms as detailed in Roebber (1984, 1989).

Context is important to understanding this concept. Consider two climates, MOIST and DRY. In the MOIST climate, the distribution of storm development features a tail skewed toward rapid development, resulting from the amplification of baroclinic dynamics by latent heating as argued throughout this paper. In the DRY climate, however, suppose that the baroclinicity is enhanced. In that case, the median of the deepening distribution may well shift toward rapid development, even if the tail is not skewed in that direction. In that case, owing to the distribution shift, there may well be as many rapidly deepening storms in DRY as in MOIST, where such storms are defined by a particular threshold of development (e.g., 1 Bergeron).

This point can be demonstrated with the 10-yr manual analysis dataset. These data are skewed but have a mean and standard deviation of 0.53 and 0.58 Bergerons, respectively. Out at the extreme deepening tail of this distribution, there are 29 cyclones that deepened at a rate of ≥ 2 Bergerons. A best-fit normal distribution produces 17 such storms, so the excess is on the order of one such cyclone per cold season. Were this normal distribution to shift 0.12 Bergerons in the mean toward rapid deepening, as was the case between CONTROL and RLHR, then this distribution, while still lacking a stretched tail, would produce 27 cyclones of at least 2 Bergerons. Thus, climatic shifts may have as much practical consequence for the occurrence of these extreme storms as the details of the rapid deepening tail.

In this work, we cannot explore the role of specific mesoscale processes in producing these developments. By the nature of the model employed, our investigations are necessarily coarse grained. Likely, details related to adiabatic and diabatic processes occurring along the warm front (e.g., Kuo et al. 1991) are critical to the history of individual events. Nonetheless, the CONTROL experiment captures the broad character of rapid maritime cyclogenesis and provides some confidence that our

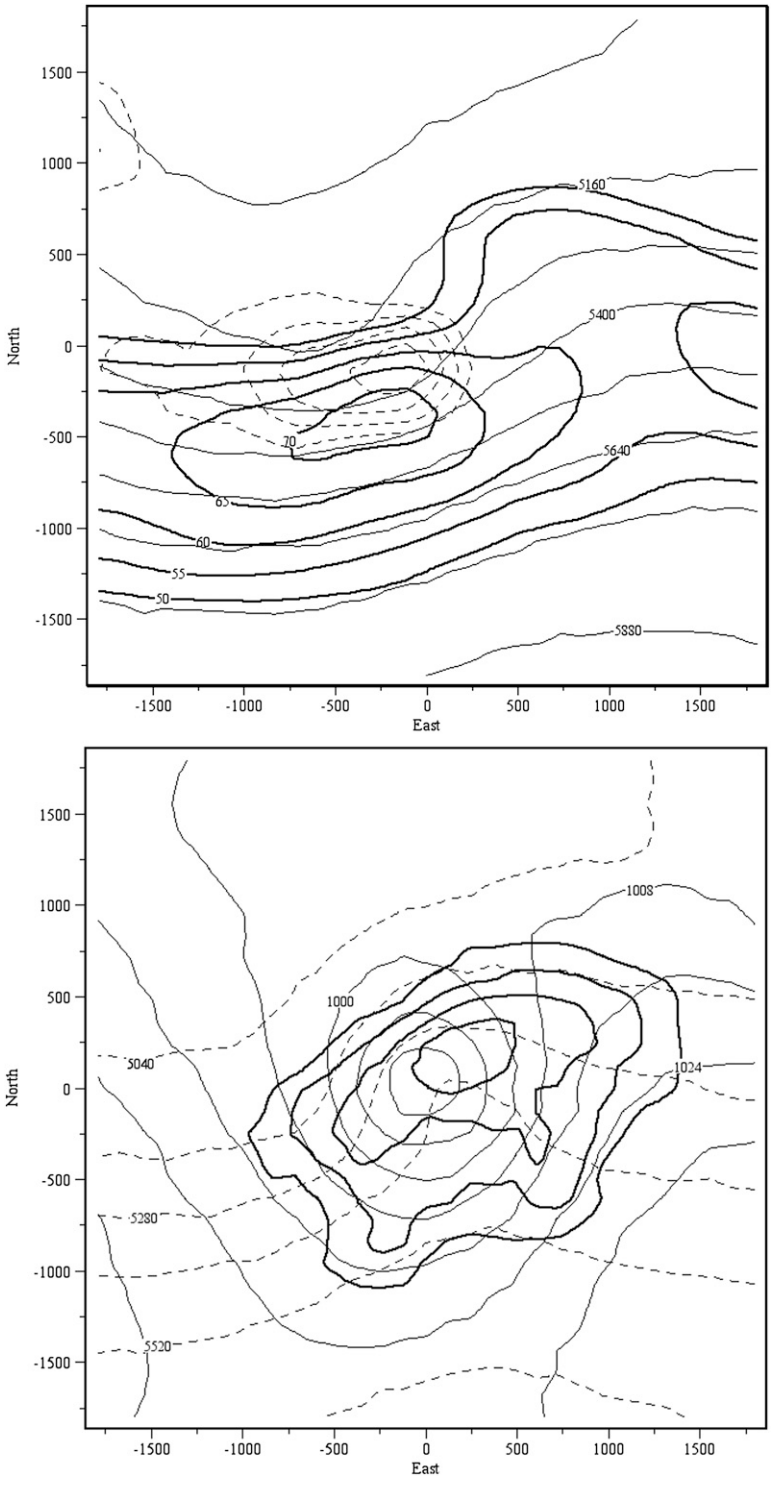

FIG. 9. Ten-case rapid deepening composite from CONTROL, centered on the cyclone center at the midpoint of the 24-h period of maximum deepening, and extending 1800 km in each direction. (top) The 500-hPa geopotential height (120 dam, thin solid), geostrophic absolute vorticity (2×10^{-5} s^{-1}, dashed, first contour 14×10^{-5} s^{-1}), and 300-hPa wind speed (thick solid, 5 m s^{-1}, first contour 50 m s^{-1}). (bottom) The sea level pressure (8 hPa, thin solid), 1000–500-hPa thickness (120 dam, dashed), and 24-h total precipitation (mm, thick solid, first contour 10 mm).

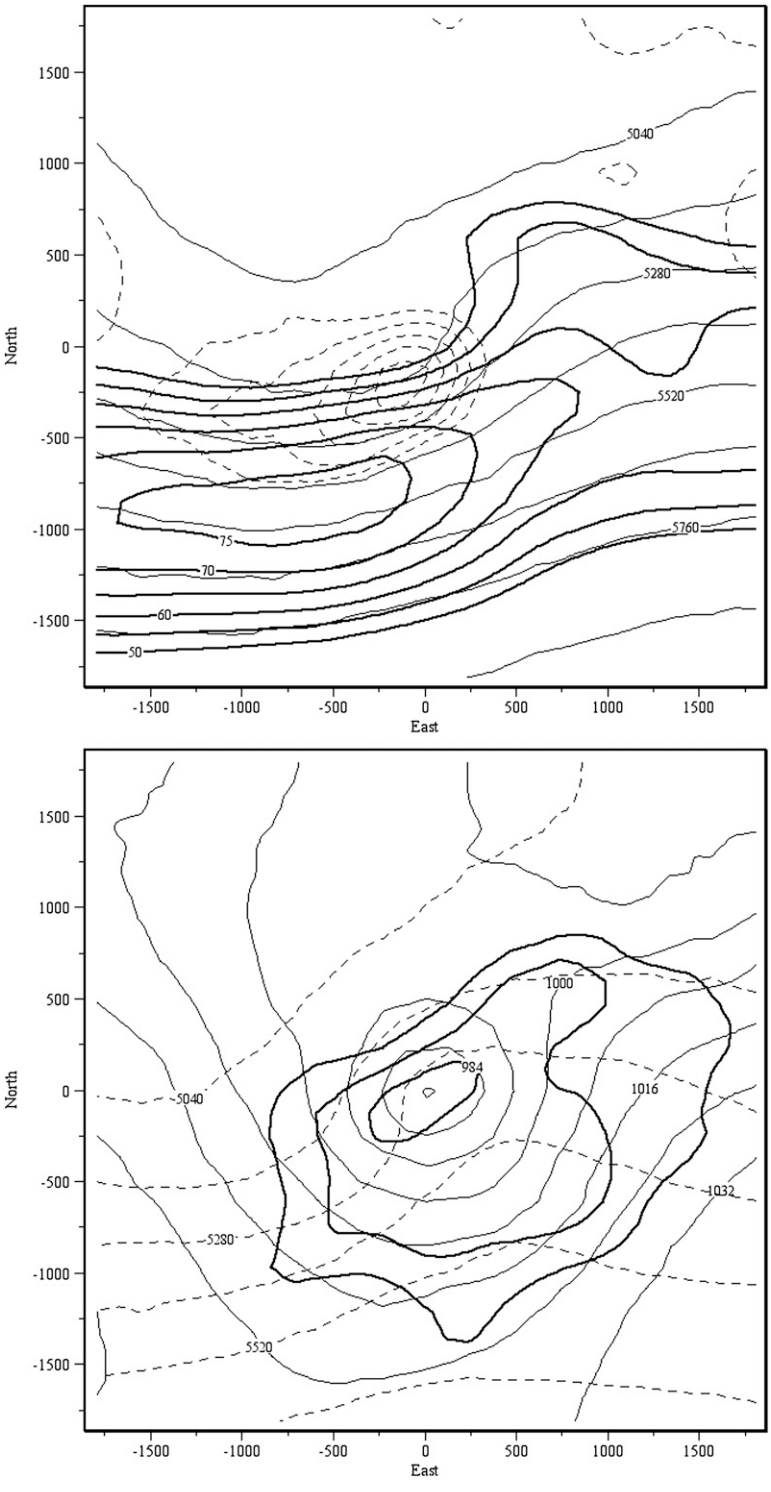

FIG. 10. Ten-case rapid deepening composite from RLHR/RAD, centered on the cyclone center at the midpoint of the 24-h period of maximum deepening, and extending 1800 km in each direction. (top) The 500-hPa geopotential height (120 dam, thin solid), geostrophic absolute vorticity (2×10^{-5} s^{-1}, dashed, first contour 14×10^{-5} s^{-1}), and 300-hPa wind speed (thick solid, 5 m s^{-1}, first contour 50 m s^{-1}). (bottom) The sea level pressure (8 hPa, thin solid), 1000–500-hPa thickness (120 dam, dashed), and 24-h total precipitation (mm, thick solid, first contour 10 mm).

experiments provide useful information concerning the physical processes that drive intense maritime systems.

4. Conclusions

We have produced a CONTROL and three additional experiments using the global version of the MM5 to analyze the role of physical processes in producing the rapid deepening tail of maritime cyclogenesis. Here, we are interested not in the behavior of individual cyclones, which can be idiosyncratic, but rather the pattern of behavior of maritime cyclones as a class. These experiments reveal that the strongest maritime storms are in some sense a ''lucky'' accident in which the strong baroclinic dynamics of the relative few are preferentially enhanced through feedbacks with the available moisture [such as with moist frontogenesis, as in Kuo et al. (1991)]. Increases in baroclinic forcing, in the absence of this moisture availability, produce substantial cyclone developments but do not produce the skewed rapid deepening tail behavior. Likewise, an increase in surface roughness in the maritime region provides only a slight brake on cyclone development. These results, in combination with the extensive literature studying individual cyclone events, provide a more complete picture of the role of physical processes in producing these prominent and dangerous systems.

A refinement of this work would be to considerably expand the cyclone databases derived from the CONTROL and RLHR experiments. Although the statistics developed here indicate a reasonable ability to distinguish nonnormal distributions, the extreme tail of the cyclone deepening distribution is populated by definition by rare events, and an expanded database constructed from two longer experimental simulations would dramatically reduce the possibility of statistical error.

Related to the extension of the model simulation is the suggestion that the model atmosphere may not have achieved a statistically steady state after 320 days of integration (e.g., Fig. 3). A t test allows us to reject the null hypothesis that the mean of the zonal jet is the same for the third and fourth quarters of these data in CONTROL. This same test, however, does not allow rejection for either the Eady growth rate maximum in the storm track entrance region or for cyclone frequencies from CONTROL. Thus, we cannot conclusively state that a statistically steady state has not been achieved, particularly for those factors of most relevance to the focus of this study. Nonetheless, an extension of these simulations would be beneficial and, given the wide availability of global models and computer processing capability, is quite feasible and will be pursued in future work.

Another technical contribution would be an improved cyclone detection-and-tracking algorithm, keyed to mimic the manual analyses reported in the extended Gyakum et al. (1989) database. A generalized, reliable method would contribute to a wide range of cyclone studies, given the ubiquity of gridded reanalysis and climate model databases.

Acknowledgments. This research is an outgrowth of 30 years of interest by PJR in rapidly deepening cyclones. We thank the many scientists who over the intervening years have worked hard to understand these events and, in so doing, have improved our collective ability to forecast them and advance maritime safety. PJR dedicates this paper in particular to three mentors who have contributed much to those several decades of research: Fred Sanders, John Gyakum, and Lance Bosart. We also thank John Gyakum for generously sharing his 10-yr cyclone tracking database, and Lance Bosart for providing thoughtful commentary on an early version of this manuscript.

REFERENCES

Blackadar, A. K., 1979: High resolution models of the planetary boundary layer. *Advances in Environmental Science and Engineering,* J. Pfafflin and E. Ziegler, Eds., Vol. 1, No. 1, Gordon and Breach, 50–85.

Blender, R., and M. Schubert, 2000: Cyclone tracking in different spatial and temporal resolutions. *Mon. Wea. Rev.,* **128,** 377–384.

Bosart, L. F., 1999: Observed cyclone life cycles. *The Life Cycles of Extratropical Cyclones,* M. A. Shapiro and S. Grønås, Eds., Amer. Meteor. Soc., 187–213.

Carlson, T. N., and F. E. Boland, 1978: Analysis of urban–rural canopy using a surface heat/flux temperature model. *J. Appl. Meteor.,* **17,** 998–1013.

Colucci, S. J., 1976: Winter cyclone frequencies over the eastern United States and adjacent western Atlantic. *Bull. Amer. Meteor. Soc.,* **57,** 548–553.

Corfidi, S. F., and K. E. Comba, 1989: The Meteorological Operations Division of the National Meteorological Center. *Wea. Forecasting,* **4,** 343–366.

Dudhia, J., 1989: Numerical study of convection observed during the Winter Monsoon Experiment using a mesoscale two-dimensional model. *J. Atmos. Sci.,* **46,** 3077–3107.

——, and J. F. Bresch, 2002: A global version of the PSU–NCAR Mesoscale Model. *Mon. Wea. Rev.,* **130,** 2989–3007.

Grell, G. A., J. Dudhia, and D. R. Stauffer, 1994: A description of the fifth-generation Penn State/NCAR Mesoscale Model (MM5). NCAR Tech. Note NCAR/TN-398+STR, 138 pp. [Available from NCAR, P.O. Box 3000, Boulder, CO 80307-3000.]

Gyakum, J. R., J. R. Anderson, R. H. Grumm, and E. L. Gruner, 1989: North Pacific cold-season surface cyclone activity: 1975–1983. *Mon. Wea. Rev.,* **117,** 1141–1155.

Haigh, J. D., 2009: Mechanisms for solar influence on the Earth's climate. *Climate and Weather of the Sun–Earth System,* T. Tsuda et al., Eds., Terra Scientific, 231–256.

——, M. Blackburn, and R. Day, 2005: The response of tropospheric circulation to perturbations in lower-stratospheric temperature. *J. Climate,* **18,** 3672–3685.

Held, I. M., M. Ting, and H. Wang, 2002: Northern winter stationary waves: Theory and modeling. *J. Climate,* **15,** 2125–2144.

Hoskins, B. J., and P. J. Valdes, 1990: On the existence of storm tracks. *J. Atmos. Sci.,* **47,** 1854–1864.

Jung, T., S. K. Gulev, I. Rudeva, and V. Soloviov, 2006: Sensitivity of extratropical cyclone characteristics to horizontal resolution in the ECMWF model. *Quart. J. Roy. Meteor. Soc.,* **132,** 1839–1857.

Klein, W. H., 1957: Principal tracks and mean frequencies of cyclones and anticyclones in the Northern Hemisphere. U.S. Weather Bureau Research Paper 40, 60 pp.

Krishnamurti, T. N., 1968: A study of a developing wave cyclone. *Mon. Wea. Rev.,* **96,** 208–217.

Kuo, Y.-H., and S. Low-Nam, 1990: Prediction of nine explosive cyclones over the western Atlantic with a regional model. *Mon. Wea. Rev.,* **118,** 3–25.

——, M. A. Shapiro, and E. G. Donall, 1991: The interaction between baroclinic and diabatic processes in a numerical simulation of a rapidly intensifying extratropical marine cyclone. *Mon. Wea. Rev.,* **119,** 368–384.

Kurz, M. E., 2009: The effects of short-term solar variability on winter climate in the Northern Hemisphere. M.S. thesis, Dept. of Mathematical Sciences, University of Wisconsin—Milwaukee, 73 pp.

Kuwano-Yoshida, A., and Y. Asuma, 2008: Numerical study of explosively developing extratropical cyclones in the northwestern Pacific region. *Mon. Wea. Rev.,* **136,** 712–740.

Mlawer, E. J., S. J. Taubman, P. D. Brown, M. J. Iacono, and S. A. Clough, 1997: Radiative transfer for inhomogeneous atmospheres: RRTM, a validated correlated-k model for the longwave. *J. Geophys. Res.,* **102,** 16 663–16 682.

Petterssen, S., 1956: *Motion and Motion Systems.* Vol. 1, *Weather Analysis and Forecasting,* McGraw-Hill, 422 pp.

Raible, C. C., P. M. Della-Marta, C. Schwierz, H. Wernli, and R. Blender, 2008: Northern Hemisphere extratropical cyclones: A comparison of detection and tracking methods and different reanalyses. *Mon. Wea. Rev.,* **136,** 880–897.

Reitan, C. H., 1974: Frequencies of cyclones and cyclogenesis for North America, 1951–1970. *Mon. Wea. Rev.,* **102,** 861–868.

Roebber, P. J., 1984: Statistical analysis and updated climatology of explosive cyclones. *Mon. Wea. Rev.,* **112,** 1577–1589.

——, 1989: On the statistical analysis of cyclone deepening rates. *Mon. Wea. Rev.,* **117,** 2293–2298.

Sanders, F., 1987: Skill of NMC operational dynamical models in prediction of explosive cyclogenesis. *Wea. Forecasting,* **2,** 322–336.

——, and J. R. Gyakum, 1980: Synoptic–dynamic climatology of the ''bomb.'' *Mon. Wea. Rev.,* **108,** 1589–1606.

——, and S. L. Mullen, 1996: The climatology of explosive cyclogenesis in two general circulation models. *Mon. Wea. Rev.,* **124,** 1948–1954.

Tabachnick, B. G., and L. S. Fidell, 2007: *Using Multivariate Statistics*. Pearson/Allyn and Bacon, 980 pp.

Tracton, M. S., 1978: Diagnosis of numerical analyses and forecasts from the perspective of quasi-geostrophic dynamics. NOAA/NWS Office Tech. Note 183, 48 pp. [Available online at www.ncep.noaa.gov/officenotes/NOAA-NPM-NCEPON-0002/013BA209.pdf.]

Uccellini, L. W., 1990: Processes contributing to the rapid development of extratropical cyclones. *Extratropical Cyclones: The Erik Palmén Memorial Volume,* C. W. Newton and E. Holopainen, Eds., Amer. Meteor. Soc., 81–105.

Whittaker, L. M., and L. H. Horn, 1981: Geographical and seasonal distribution of North American cyclogenesis. *Mon. Wea. Rev.,* **109,** 2312–2322.

Zhang, D., and R. A. Anthes, 1982: A high-resolution model of the planetary boundary layer-sensitivity tests and comparisons with SESAME-79 data. *J. Appl. Meteor.,* **21,** 1594–1609.

Zishka, K. M., and P. J. Smith, 1980: The climatology of cyclones and anticyclones over North America and surrounding ocean environs for January and July, 1950–77. *Mon. Wea. Rev.,* **108,** 387–401.